Grain size modelling of a low carbon strip steel during hot rolling in a Compact Strip Production (CSP) plant using the Hot Charge Route

by W. Stumpf*

Synopsis

Mill log analyses and complementary hot deformation studies were carried out on the as-cast structure and on a hot rolled structure of the same low carbon steel (SAE 1006) that had been processed according to the direct or hot charge route in a compact strip plant. The main softening mechanisms during hot rolling were found to be complete dynamic recrystallization during each pass above about 1000°C for the as-cast structure with an austenite grain size of 277 µm and, secondly, incomplete static recrystallization after each pass with a finer austenite grain size of about 26 µm and tested below 1000°C. A two-stage hot working mechanism has also been found by others on a similar steel also processed by the hot charge route and this may appear to be a characteristic of this type of material. Constitutive constants determined from hot working studies were combined with other constants from the literature and incorporated into a grain size development model that correctly predicts the final ferrite grain size in the hot rolled strip steel. The predicted incomplete static recrystallization during the last three finishing passes in the plant appears to result in some retained strain in the hot rolled austenite as it transforms to ferrite on the run-out table. Analyses with the model predict relatively little sensitivity of the final ferrite grain size to process and product variables such as temperature and strain per pass for the last three passes and also the starting austenite grain size in the slab.

Keywords: Low carbon steel, hot rolling of strip steel, rolling mill log analyses, austenite grain size, ferrite grain size, grain size modelling.

Introduction

Many modern and compact strip mills for carbon and low alloy steels are of the so-called 'mini' design in which *inter alia* the slab, after continuous casting, is sent directly to the reheat furnace for temperature equalization while within the austenite phase before hot rolling. This is in contrast to most older conventional strip mills where the cast slab is allowed to cool to room temperature in the ferrite phase first before reheating to austenite and then hot rolling. The former process is, therefore, often called the hot charge route (HCR) as opposed to the cold charged route (CCR) of a conventional plant. In South Africa ISCOR (Saldanha) is an example of a compact strip production plant of HCR-design, whereas ISCOR (Vanderbijlpark) operates a CCR-designed plant, both for the production of carbon and low alloy strip steel to hot rolled thicknesses of less than 2 mm.

Other process differences (and hence possible product differences) may also exist between the two classes of strip mills. Modern CSP strip mills are usually designed very compactly with less hot rolling stages than conventional plants and mostly start from a thinner continuously cast slab. For instance, the ISCOR (Saldanha) plant operates with only two roughing passes in tandem and five finishing passes in tandem for starting slab thicknesses of 75 or 90 mm, whereas the ISCOR (Vanderbijlpark) plant would be able to use any number of roughing passes (typically between 5 and 7) with a double reversing roughing mill and up to seven finishing passes in tandem, starting with a slab thickness of 240 mm. ISCOR (Saldanha) also applies a calcium treatment to the liquid steel that results *inter alia* in much lower sulphur contents than the ISCOR (Vanderbijlpark) product. Greater use of electric arc furnace melting in any of the two types of plant may also result in differences in the nitrogen content of the two types of steel.

In view of the many differences between the two processes it is, therefore, not likely that hot rolled HCR-strip from a compact strip mill would necessarily have the same properties as the nominally equivalent CCR-material. Very few systematic studies of differences between the low carbon hot rolled strip steels of the two types of plant have been published. The most extensive comparative study is probably the quantitative hot deformation work of Muojekwu *et al.*[1] whilst Frawley *et al.*[2] simulated both the HCR and

* *Department of Materials Science and Metallurgical Engineering, University of Pretoria, Pretoria. E-mail: wstumpf@postino.up.ac.za*

 SA ISSN 0038–223X/3.00 + 0.00. Paper received Jul. 2003; revised paper received Oct. 2003.

CCR process through hot rolling of laboratory cast ingots of low carbon manganese steels with varying sulphur contents.

Considering only the differences in the hot rolling schedules, Muojekwu *et al*. found that in a HCR-produced strip, if compared to a conventionally CCR-produced strip, the effects of through-thickness strain and strain rate variations on the development of the austenite grain size during hot rolling, are more prominent in the former. The finishing austenite grain size before transformation to ferrite on the run-out table was found to be finer in the HCR-process, leading to a finer ferrite grain size in the final product. They also pointed out that the following additional differences need to be considered:

- an entry austenite grain size of the cast slab of about 1000 µm in the HCR-material compared to the conventional about 250 µm grain size;
- higher reductions per pass with generally lower strain rates, may lead to dynamic recrystallization (DRX) in the HCR-product as opposed to the conventional more modest reductions per pass at higher strain rates that would favour static recrystallization (SRX) in a CCR-plant;
- aluminium and nitrogen remain in solution during the reheating of the slab in the case of an HCR-process, whereas AlN needs to be re-dissolved during the ingot's reheating in conventionally produced strip. The subsequent precipitation of the AlN during hot rolling of HCR-strip may then retard recrystallization and refine the austenite grain size; and
- mechanical properties may differ by differences in chemistry, ferrite grain size, any free nitrogen, as well as possible differences in MnS precipitation. In particular, the possibility of finer AlN precipitates in HCR-product that will lead to a higher strength, needs to be considered.

Frawley *et al.*[2] studied an 0.04%C–0.25%Mn steel with the sulphur content varying from 0.005 to 0.04% and in which true HCR conditions were approximated by respective cold and hot stripping the laboratory casts before hot rolling from 15 to 3.7 mm thickness in three passes, starting at 1100° and down to 900°C for the last pass. The HCR-produced steel had a finer ferrite grain size than the CCR-samples at all sulphur levels and the HCR-samples also had a higher strength than the CCR-samples but only at the higher sulphur levels exceeding 0.02%S. It was also observed that the HCR-samples had a less uniform ferrite grain size distribution than the equivalent CCR-samples. The conclusion by these authors was that the increased strength of the HCR-samples was due not only to a finer ferrite grain size but also that strain-induced MnS precipitation in these samples was also a contributing factor.

With the introduction of the ISCOR (Saldanha) plant some years ago alongside the conventional hot rolled strip producing plant of ISCOR at Vanderbijlpark, nominally the same product but produced by different processes, indicated that initially the two products differed in physical and mechanical properties. The HCR-product had a slightly smaller ferrite grain size, a slightly higher yield and tensile strength and possibly a somewhat different cold work and recrystallization behaviour than the equivalent CCR-product. These differences, however, often fell within the range of scatter for any large-volume production of most steels. A study on the two process/product combinations has, therefore, been initiated that is aimed at the following four major areas:

- A more detailed study of the HCR hot rolling process for the production of SAE 1006 strip at the ISCOR (Saldanha) plant with the establishment of a hot rolling model that predicts the austenite grain size evolution during the hot rolling process.
- A comparison between the respective HCR and CCR hot rolling processes through process and product modelling;
- A detailed study of the austenite-to-ferrite transformation in both products and how this transformation may be affected by any differences in the two steelmaking processes; and
- A study of the recrystallization behaviour after cold rolling of hot rolled strip produced by the two respective processes.

This publication addresses only the first objective and the remaining three will be addressed in later publications.

Overview of the HCR hot rolling process at ISCOR (Saldanha)

When this study was undertaken, it was practice that the steel is continuously cast into 75 mm thick slabs by a thin slab casting process, is then sectioned into shorter lengths and these enter the reheating roller hearth furnace directly for temperature equalization from where they exit at typically 1140°C before entering the two-stand roughing mill. After the roughing reductions, the transfer bar is temperature equalized once more in a coil box before entering the five-stand tandem finishing mill, where after the strip is cooled by water sprays on a relatively short run-out table before

Table I

Typical hot rolling process parameters for 2 mm hot rolled SAE 1006 strip produced from a 75 mm cast slab and hot rolled by the HCR process

Parameter	RHF	R1	R2	Coil Box	F1	F2	F3	F4	F5	FMH
Thickness in (mm)	75	75	40	22	22	11	5.6	3.8	2.7	2.0
Thickness out (mm)	75	40	22	22	11	5.6	3.8	2.7	2.0	2.0
Temperature (entry into pass) (°C)	1140	1140	1110	1040	1040	1000	970	950	920	900
Nominal strain per pass	-	-0.72	-0.69	-	-0.80	-0.78	-0.45	-0.39	-0.35	-
Nominal strain rate per pass (s^{-1})	-	-7.6	-17.6	-	-17.8	-44.9	-72.0	-117	-152	-

Notes: RHF=Reheat Furnace and FMH=Finishing Mill Head. Strains per pass ε and strain rates per pass $\dot{\varepsilon}$ were calculated according to the formulae in Appendix 1. Typical cooling rates under the water sprays of the run-out table of the final strip after finish rolling, were about 80°C/s at the time of this study.

entering the final coil box for coiling. Typical parameters for the production of a 2 mm strip of low carbon SAE 1006 steel hot rolled from a 75 mm slab in this plant at the time of this study, are given in Table I. It should, however, be noted that ISCOR (Saldanha) have since adopted an increased slab thickness of 90 mm for 2 mm hot rolled strip and have also adapted the cooling process on the run-out table and the coiling practice to optimize the product properties.

Calculating the Mean Flow Stress of the HCR SAE 1006 steel from mill logs

The Mean Flow Stress (MFS) of the material at each rolling pass was calculated by an equation first proposed by Sims[3] from the recorded mill load data taken from the mill logs. Corrective calculations included the effects of elastic roll flattening [3,4], redundant strain[5] and forward slip[6] and were incorporated into a model similar to that proposed by Siciliano *et al.*[7]. The equations used in this part of the model have been included in Appendix 1.

Ten sets of mill logs were obtained from ISCOR (Saldanha) from hot rolling schedules of 2 mm hot rolled SAE 1006 strip steel from 75 mm continuously cast slabs. The calculated MFS values for each pass are shown in Figure 1 as a function of the reciprocal absolute temperature 1/T. All MFS values have been corrected to a constant strain per pass of 0.4 and a constant strain rate per pass of 5 s^{-1} by the Misaka[8] corrections. The approximate positions of the two roughing passes R1 and R2 and the five finishing passes F1 to F5 are shown in relation to the temperature data in the Figure.

It appears that the results may lie in two separate groups with relatively low MFS values from the two roughing passes R1 and R2 as well as the first two finishing passes F1 and F2 and with an apparently lower temperature sensitivity than the data from the last three finishing passes F3 to F5. These data suggest that two different softening mechanisms might operate at temperatures typically above and below 1000°C, leading to relatively low operating mill loads above this temperature. Using data and constants from the literature for the hot rolling of low carbon strip steel (principally equations derived by Sellars and co-workers[9–13]), some initial

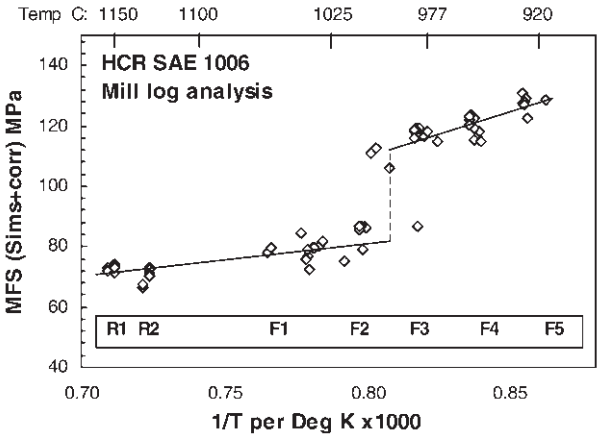

Figure 1—The Mean Flow Stress (in MPa) from mill logs as a function of the reciprocal absolute temperature 1/T (in K^{-1}) of the low carbon steel SAE 1006 and processed by the HCR-route

calculations showed that it might indeed be dynamic recrystallization (DRX) that is likely at the higher temperatures (this would lead to lower MFS values or lower mill loads as some softening is taking place within the rolls) and that static recrystallization (SRX) possibly occurs at lower temperatures. The latter would naturally lead to higher measured mill loads as softening of the steel only takes place after exiting from the rolls.

Mill log data are, however, quite notorious for their scatter, particularly arising from the temperature data that are mostly calculated by a proprietary model of the hot rolling mill vendor. Secondly, the constitutive equations used in the initial calculations make use of many material constants that were derived from slightly different steels and almost exclusively for CCR strip steels. To overcome these uncertainties, an experimental hot working programme was undertaken in which a limited number of the constitutive constants were determined under controlled conditions on a SAE 1006 steel produced at ISCOR (Saldanha) by the HCR-process.

The hot deformation of low carbon steels

The hot rolling of low carbon strip steel has received significant attention from many researchers and has led to a number of approaches[14] towards semi-empirical constitutive modelling of both the austenitic and the ferritic grain size during and after the rolling process. All approaches depart from an initial decision-making step on the fundamental softening mechanism that is encountered at each pass. In low carbon steels these softening mechanisms are normally limited to either DRX or SRX, with subsequent grain growth after softening. Dynamic Recovery (DRV) normally plays a very minor part in low carbon steels and its effect is usually ignored.

The two primary equations that quantify a metal's hot deformation behaviour are, firstly, an expression that relates the steady state flow stress to the absolute temperature and the strain rate through the so-called universal creep and hot deformation equation[15,16] and, secondly, an expression that predicts the minimum or critical strain required to initiate DRX[17]:

$$\dot{\varepsilon}\, exp(Q/RT) = Z = A_3\, [sinh(\alpha\sigma_{ss})]^n \qquad [1]$$

and $$\varepsilon_c = A_1 (D_0)^m Z^q \qquad [2]$$

where $\dot{\varepsilon}$ is the strain rate in s^{-1}, Q is the activation energy of the rate controlling softening mechanism in $J.mol^{-1}$, T is the absolute temperature of hot working in K, R is the universal gas constant in $J.mol^{-1}.K^{-1}$, A_3 and A_1 are structure factors which are assumed to be constant if one applies steady state flow stress conditions, α is a material constant, σ_{ss} is the steady state flow stress in MPa, D_0 is the initial grain size (in μm) at the start of the hot deformation test and Z is the Zener-Holloman parameter[18] with units s^{-1}. The dimensionless exponents n (also called the stress sensitivity), m and q are normally considered to be constant with temperature.

The critical strain ε_c necessary for the initiation of DRX is a rather difficult parameter to measure, and Equation [2] usually incorporates the peak strain ε_p from the flow stress curve and this strain relates to the critical strain for DRX

Table II

Composition of the as-cast SAE 1006 steel processed by the HCR-route and used in the hot deformation tests

%C	%Mn	%Si	%Al(sol)	%Al(tot)	%Cr	%Ni	%V
0.038	0.25	0.02	0.037	0.045	0.008	0.001	0.007
%Ti	**%Nb**	**%Cu**	**%Mo**	**%P**	**%Ca**	**S ppm**	**N ppm**
0.001	0.002	0.009	<0.001	0.005	0.002	1.8	65

through a well proven relationship of $\varepsilon_c = 0.8\varepsilon_p$ for low carbon steels[17]. Researchers on inter *alia low* carbon strip steel that was mostly processed by the conventional CCR process, have determined values for practically all of the above constants and exponents with some minor, but also with some significant differences, in some of the values. In view of the above 'two-level' MFS results in Figure 1 of the HCR-processed SAE 1006 steel strip derived from an analysis of the mill logs, it was felt to be prudent to determine at least the above constants in Equations [1] and [2] through hot deformation tests and not to rely necessarily only on published constants.

Experimental hot working programme

SAE 1006 steel used in the hot working tests

The steel used for the test programme was HCR-processed SAE 1006 steel cut from a cast 75 mm slab with the composition shown in Table II.

The very fact that this HCR steel, although in the as-cast condition, had already been cooled once through the austenite-to-ferrite transformation temperature before testing, made it, strictly speaking, not a true test of the hot charging process any more. This fact, also realized by Muojekwu *et al.*[1], underlines the real difficulty of simulating full plant conditions exactly in such hot deformation studies. The chemistry of the steel was nevertheless fully representative of the true HCR-steel. To circumvent this unavoidable difference from actual plant conditions, a relatively high soaking temperature of 1200°C was used before the start of the hot deformation tests in an attempt to fully dissolve the AlN precipitates, as is the case in a true HCR process. This temperature exceeds the solubility limit for the particular nitrogen and total aluminium contents of this steel from Table II, which was calculated[19] as 1082°C.

The above steel was tested under two different conditions, firstly in the as-cast condition with a relatively large austenite grain size and tested above 1000°C and, secondly, in the hot rolled condition with a much smaller austenite grain size and tested below 1000°C. The smaller grain size was achieved by hot rolling the as-cast sections from 40 mm thickness to 12 mm thickness in four reduction passes in a laboratory mill starting at 1200°C for the first pass and ending at 1000°C for the last of four passes.

Starting austenite grain sizes

To determine the starting austenite grain size in these very low carbon steels that possess virtually no hardenability, a hyper-eutectoid carburization method was developed based on the standard McQuaid-Ehn[20] test. On two samples, the austenite grain size was first stabilized at the starting temperature for the later hot deformation test under Argon (1200°C for the as-cast structure and 1000°C for the hot rolled material) before carburizing the sample with CO gas at 925°C for 8 hours to hypereutectoid carbon levels. Slow cooling to below 600°C allowed the pro-eutectoid Fe_3C to decorate the prior austenite grain boundaries, making them suitable for grain size measurements by the mean intercept method. The as-cast microstructure conditioned at 1200°C for 3 minutes had a prior austenite grain size of 277 μm, whereas that of the hot rolled material conditioned at 1000°C was 26 μm. Testing for grain size uniformity by the relationship proposed by Thompson[21] of (largest grain diameter)/(mean intercept length) = 1.86 for a fully uniform microstructure, lead to typical values between 2 and 2.3, indicating a reasonably uniform austenite grain size distribution. Figure 2 shows the decoration of the prior austenite grain boundaries by this technique in the as-cast material.

Hot deformation tests

The hot deformation tests were carried out on 10 mm diameter by 15 mm long cylindrical samples on a Gleeble 1500^{TM} machine fitted with a specially constructed load cell fitted to the stationary part of the load application train. This reduced the machine frictional forces to typically less than 1.5 percent of the measured load on the sample. Samples were first soaked at 1200°C for 3 minutes for the coarse grained as cast structure and 1000°C for the hot rolled smaller grain size structure before lowering the temperature to the test temperature and applying the programmed strain and strain rate. The latter ranged from 0.001 s^{-1} to 3 s^{-1} and the applied strain was limited to about 0.47 true strain to avoid excessive barrelling, with barrelling coefficients[22] generally above 0.87. In analysing the measured flow stress curves, a friction coefficient between the sample and a Ta foil on the two WC pressure anvils of 0.2 was assumed[23,24] and

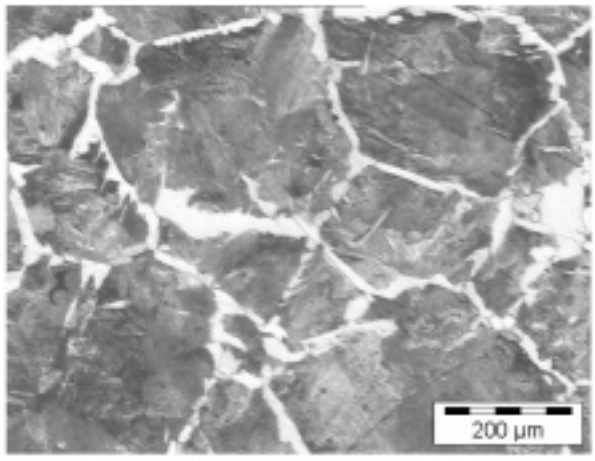

Figure 2—Prior austenite grain size structure at 1200°C of the SAE 1006 low carbon steel processed by the HCR-route and in the as-cast condition. The prior austenite grain boundaries at 1200°C have been decorated by cementite through hyper-eutectoid carburization. Etchant used: 2% Nital

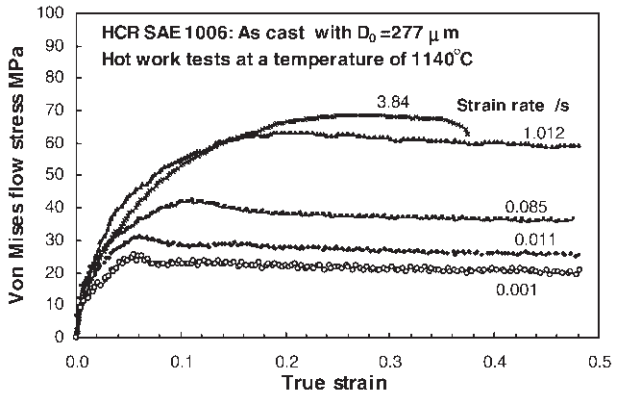

Figure 3—High temperature flow stress curves of as-cast HCR-processed SAE 1006 steel, tested at 1140°C at different strain rates

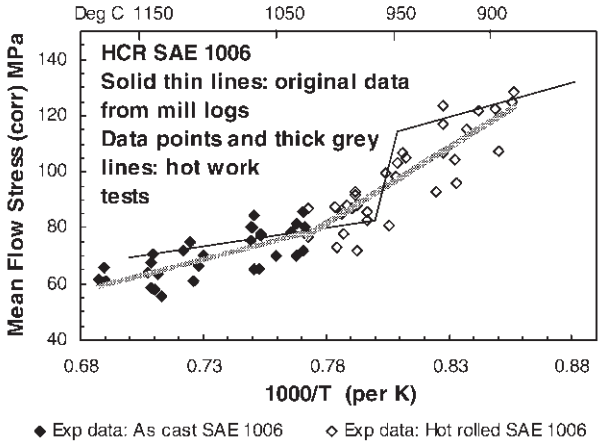

Figure 4—Mean Flow Stress values determined from hot deformation tests and plotted on the mill log derived lines from Figure 3 for both the HCR as-cast coarse grained material (filled symbols) and the finer grained hot rolled material (open symbols)

the Von Mises flow stress calculated from the expression given by Dieter[25] and originally developed by Rowe[26]. From these corrected flow stress curves the steady state flow stress σ_{ss} and the peak strain ε_p were read off and the mean flow stress calculated from the entire curve[27].

From Equations [1] and [2] the constant Q may be determined from a series of tests at different temperatures (by plotting $ln[sinh(\alpha\sigma_{ss})]$ versus $1/T$) but at constant strain rates whereas the stress sensitivity n of Equation [1] needs to be determined first by plotting ($ln[sinh(\alpha\sigma_{ss})]$ versus $ln\ Z$) from a series of tests at various temperatures and strain rates. Tests on the as-cast large austenite grain size material were restricted to temperatures above 1000°C, whereas the hot rolled smaller grain size material was used for all tests below 1000°C. This distinctive temperature was derived from Figure 1 where this temperature also appears to be the dividing line between the two regimes of MFS data obtained from the plant's mill logs.

Experimental results

Typical flow stress curves

Some typical flow stress curves at various strain rates for the as-cast HCR-steel are shown in Figure 3. The drop in flow stress to steady state conditions after reaching a peak stress first, which is typical of DRX taking place during the test, was present in practically all tests, even those at the lower temperatures with the finer grain size material.

Mean Flow Stress results from both sets of material

In Figure 4 the MFS values from the hot working tests on both the as-cast coarse grained (filled symbols) as well as the hot rolled and finer grained material (open symbols) are shown together with the two mill log lines from Figure 1. In all cases the MFS was corrected to a constant strain of 0.4 and a constant strain rate of 5 s^{-1} per pass. In general, the levels of MFS from the hot work tests correlate reasonably well with those calculated independently from the plant's mill logs with the MFSs of the two differently grain sized specimens linking up at about 1000°C but apparently following different temperature sensitivity paths.

MFS values, even those measured under well controlled conditions, will result in more scatter as they measure an integrated value of the entire flow stress curve which contains regions of both strain hardened as well as softened material. This is unlike the more precisely defined steady state stress σ_{ss} of Equation [1] where a balance between strain hardening and strain softening in the material has been reached.

Constitutive constants for both sets of HCR-steel

Considering both Equations [1] and [2], one needs to plot first a figure of $[ln\ \dot{\varepsilon}]$ versus $[ln[sinh(\alpha\sigma_{ss})]]$ at constant temperatures to find an initial value for the stress sensitivity n from the slopes of the curves. These initial curves are not shown here. Thereafter one may plot the three curves shown in Figure 5 for the as-cast coarse grained structure depicting basically Equations [1] and [2] from which the constants Q, m, A_1, A_3, q and n (once more) for that particular material may be determined.

In a similar manner the constitutive constants for the fine-grained material tested below 1000°C are shown in Figure 6 and a summary of all these constants, together with the equivalent constants from the literature for low carbon steels, are shown in Table III.

It is interesting to note that Muojekwu *et al.*[1] who used HCR-steel with a composition of 0.17%C – 0.74%Mn, also predicted a different softening behaviour between large and smaller grain sized material with a cut-off point at about 244 μm and an activation energy of about 202 kJ/mol for Equation [2]. These authors, however, proposed an additional decision-making step to test for DRX beyond the normal $\varepsilon > \varepsilon_c$ of Equation [2] by introducing a further decision of whether the actual strain rate $\dot{\varepsilon}$ was greater or smaller than a specially derived steady state strain rate ε_{ss}. They proposed that the latter was dependent on both austenite grain size and temperature, but with a different temperature dependence or activation energy for grain sizes below 244 μm and above.

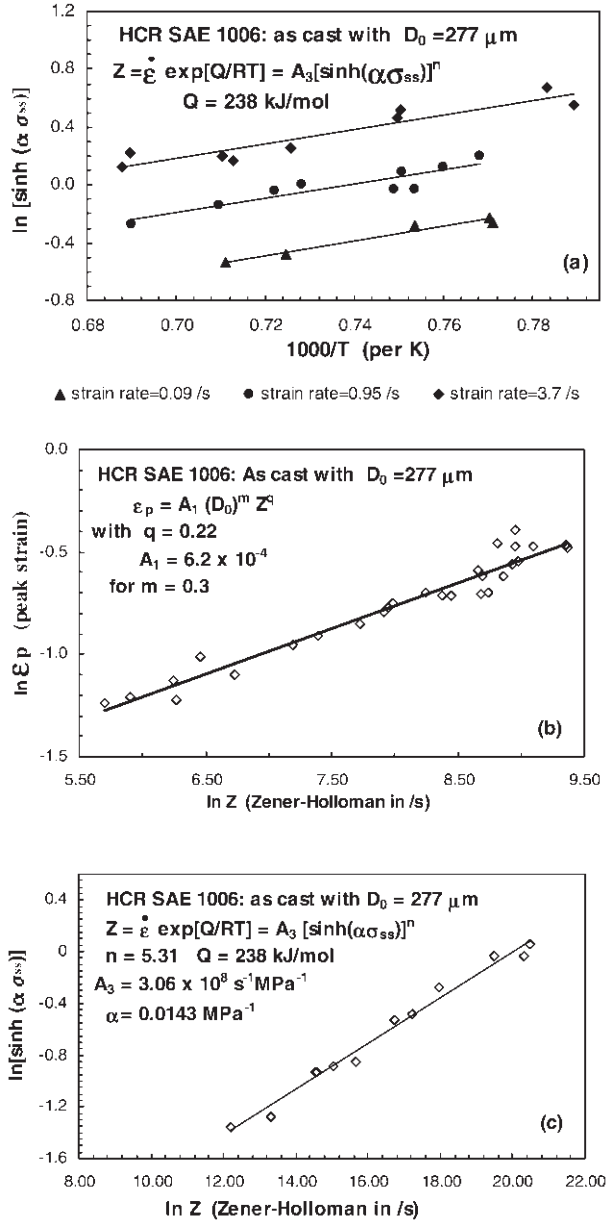

Figure 5—Hot deformation curves for the HCR as-cast coarse grained SAE 1006 steel with the curve (a) used to find the activation energy Q from Equation [1], (b) used to find the values for *q* and A_1 from Equation [2] and (c) the overall hot deformation curve combining all of the data in terms of Equation [1]. Line fitting: regression coefficients R^2 were larger than 0.950 in all cases except for the top line in Figure (a) where R^2 = 0.905

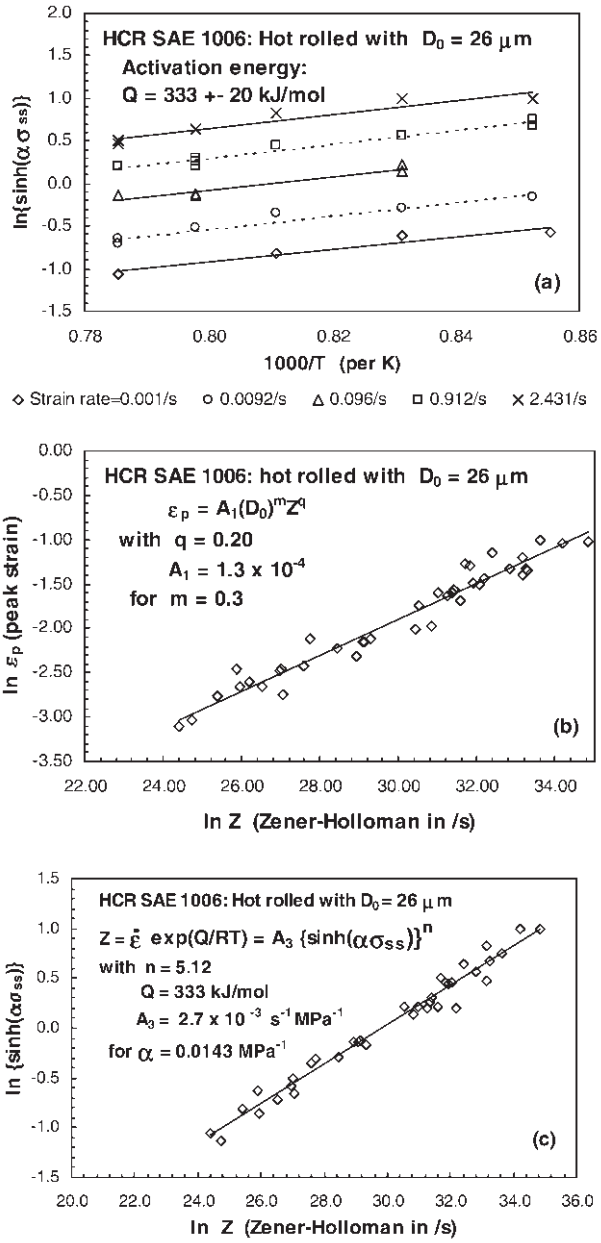

Figure 6—Hot deformation curves for the HCR hot rolled and fine grained SAE 1006 steel with the curve (a) used to find the activation energy *Q* from Equation [1], (b) used to find the values for *q* and A_1 from Equation [2] and (c) the overall hot deformation curve combining all of the data in terms of Equation [1]. Line fitting: regression coefficients R^2 were larger than 0.950 in all cases

Grain size development model

Many authors have proposed semi-empirical models that predict the austenite grain size development during hot rolling. For low carbon strip steel the models generally incorporate decision-making elements of DRX within the rolls and SRX plus grain growth during the interpass times with a wide variation in the exact equations used. In this work the well-proven approach of Sellars and his co-workers[9-13, 16, 17] and also largely used by Jonas and his co-workers[7, 23, 24, 30] was used as a basis for the austenite grain size development model. The IRSID equation[33] was used for the ferrite grain size with this expression being one of a small number of empirically determined transformation equations that incorporate an alloy factor for carbon and manganese, thereby allowing some comparison between separate but similar steels. The decision-making model established for this study is shown in Appendix 2 for the austenite grain size development. The experimentally determined constitutive constants from Table III were introduced into the model, while the more widely accepted constants from the literature for low carbon strip steel were used in the remaining cases. The equations used in the decision-making model are shown in Appendix 3.

The model soon showed that incomplete static recrystallization (SRX) was predicted to take place in the interpass

Table III

Summary of the constitutive constants determined in this study and compared to some typical values from the literature. (Note that in this table ε_p is used instead of ε_c for Equation [2] with $\varepsilon_c = 0.8\varepsilon_p$)

Material	$\dot{\varepsilon}\exp(Q/RT) = Z = A_3 \sinh(\alpha\sigma_{ss})\}^n$	$\varepsilon_p = A_1(D_0)^m Z^q$
HCR as-cast SAE 1006 steel tested at T > 1000°C and for an austenite grain size D_0 = 277 μm	Q = 238 kJ/mol at T > 1000°C n = 5.3 $A_3 = 3.8\times10^8$ $s^{-1}MPa^{-1}$	q = 0.22 $A_1 = 6.2\times10^{-4}$ for D_0 = 277 μm
HCR hot rolled SAE 1006 steel tested at T < 1000°C and for an austenite grain size D_0 = 26 μm	Q = 333 ±20 kJ/mol at T < 1000°C n = 5.1 $A_3 = 1.25\times10^{13}$ $s^{-1}MPa^{-1}$	q = 0.20 $A_1 = 1.3\times10^{-4}$ for D_0 = 26 μm
Typical values from the literature for low carbon strip steel For *Q* see refs. 1, 7, 10 and 29 For *n* see refs. 1, 32 For A_1 see refs. 1, 7, 10, 31, 32 For A_3 see ref. 1 For *q* see refs. 7, 10, 30-32 For *m* see refs. 1, 7, 10, 30, 31 For α see refs. 1, 28, 32	Q = 202 to 314 kJ/mol with 312 accepted widely n = 4.34 to 5.3 $A_3 = 9.69\times10^{11}$ $s^{-1}MPa^{-1}$ α = 0.0095 to 0.0143 MPa^{-1} with 0.0143 accepted widely	q = 0.17 to 0.23 m = 0.1 to 0.5 with 0.3 accepted widely $A_1 = 4.6\times10^{-4}$ to 1.3×10^{-2}

times during the last three passes of F3, F4 and F5 on the plant, and the following equation that incorporates 'strain-on-strain-on-strain' during these passes was developed and introduced into the model to follow the accumulated strain over the last three passes up to the FMH.

$$\varepsilon_r = [X_3X_4(1-X_5)\varepsilon_5] + [X_3(1-X_4)(1-X_5)(\varepsilon_4+\varepsilon_5)] + [(1-X_3)X_4(1-X_5)\varepsilon_5] + [(1-X_3)(1-X_4)(1-X_5)(\varepsilon_3+\varepsilon_4+\varepsilon_5)] \quad [3]$$

where X_3, X_4 and X_5 are the calculated volume fractions of recrystallized (by SRX) material after the interpass times after passes F3, F4 and F5 respectively (with 0.5 s taken as the exit time between F5 and the FMH) and ε_3, ε_4 and ε_5 are the true strains applied during passes F3, F4 and F5 respectively. The derivation of Equation 3 is based on a unit volume of fully recrystallized (by DRX) material that enters pass F3 and which thereafter splits up into at least eight different populations after pass F5, four with no accumulated strain (where SRX was complete) and four populations with differing amounts of 'strain-on-strain' where the recrystallization was incomplete.

In principle, the grain size development model consists of a number of sections that make use, firstly, of input data per pass, secondly of calculated intermediate data per pass, and finally of output data per pass, such as:

- *Required input data per pass*: elastic moduli of the rolls, roll diameters, intermediate product thicknesses (in), intermediate product thicknesses (out), plate or strip widths, entry temperatures into the pass and average temperatures within the rolls, mill loads of rolling during each pass, interpass times and the roll speeds;
- *Calculated process data per pass*: this includes the roll flattened radius, redundant strain, forward slip factor or ratio, nominal strain, total strain (which includes the redundant strain), strain rate (which corrects for forward slip), Zener-Holloman parameter, the Mean Flow Stress and the MFS as corrected for a constant strain and strain rate per pass; and
- *Predicted product data per pass*: this includes: austenite grain size, critical strain for DRX, strain for 50% DRX, fraction softened by DRX, grain size from DRX, grain growth after DRX, time for 50% SRX, accumulated strain at incomplete SRX, austenite grain size from SRX, grain growth after SRX, retained strain at the last pass resulting from any prior incomplete SRX passes, austenite grain size at the FMH in the final product at 0.5 seconds out of the last pass F5, ferrite grain size from the SRX population after the FMH, ferrite grain size from the incompletely recrystallized populations and the final predicted ferrite grain size mix in the final product before coiling.

This HCR-model may be applied to any reduction schedule for low carbon strip steel at the ISCOR (Saldanha) plant with the following typical example in Table IV for a slab of 75 mm thickness that had been rolled down to a 2 mm strip through two roughing and five finishing passes and with a soaking temperature of the slab of 1137°C and a finishing temperature of 893°C.

The following may be noted from this typical and other calculated examples:

- The calculated final ferrite grain size of 9.7 μm agrees very well with the measured ferrite grain size for this particular strip of 9.5 μm.
- Full DRX takes place within the passes R1 to F2 and thereafter only partial SRX takes place after the passes F3 to F5. This is in agreement with the mill log analyses in Figure 1 that have shown a sudden increase in the measured MFS between passes F2 and F3. It is interesting to note, however, that in the hot working tests at typical temperatures of passes F3 to F5 but at slower strain rates (the maximum strain rate was 2.5 s^{-1} for the low temperature tests) DRX was found to occur in the hot working tests. At the much higher strain rates in the plant in these same passes, however, the resulting higher value of *Z* correctly predicts SRX with incomplete softening taking place during the F3 to F5 reductions.

Table IV

Typical process and product parameters predicted by the model for a 75 mm slab hot rolled down to 2 mm HCR-strip which had a measured final ferrite grain size of 9.5 μm. The cooling rate on the run-out table was taken as 80°C s^{-1}

Process input data	**R1**	**R2**	**F1**	**F2**	**F3**	**F4**	**F5**	**FMH**
Entry thickness (mm)	75	40.1	21.8	10.8	5.6	3.8	2.7	2.0
Plate width (mm)	1293	1302	1313	1313	1313	1313	1313	1313
Entry temperature (°C)	1137	1113	1033	1004	955	947	921	893
Roll separating force (MN)	20.3	18.1	20.3	19.9	16.7	13.4	11.2	
Interpass time to next pass (s)	4.2	30.0	3.5	1.8	1.2	0.8	0.5	
Roll circumferential speed (m/s)	1.29	2.36	1.61	3.08	4.68	6.58	8.62	
Process output data	**R1**	**R2**	**F1**	**F2**	**F3**	**F4**	**F5**	**FMH**
Total strain per pass	0.79	0.75	0.85	0.78	0.48	0.40	0.31	
Strain rate per pass (s^{-1})	7.7	17.6	17.81	44.9	72.0	116.6	151.6	
Zener-Holloman (s^{-1})	5.01 E+09	1.62 E+10	5.80 E+10	2.43 E+11	7.97 E+15	2.09 E+16	5.49 E+16	
MFS corrected to 0.4 strain and 5 s^{-1} strain rate (MPa)	73.1	66.5	78.1	80.3	111.0	116.3	115.3	
Predicted product data	**R1**	**R2**	**F1**	**F2**	**F3**	**F4**	**F5**	**FMH**
Entry austenite grain size (μm)	277	152.7	116.6	87.0	62.6	31.1	26.8	
Critical strain for DRX	0.37	0.34	0.41	0.52	0.48	0.44	0.52	
DRX/SRX softening during/after pass?	DRX	DRX	DRX	DRX	SRX	SRX	SRX	
Fraction softened by DRX	1	1	1	1				
Grain size from DRX (μm)	152.7	116.6	86.9	62.6				
Fraction softened by SRX					0.89	0.98	0.56	
Austenite grain size from SRX (μm)					31.1	22.9	22.9	
Austenite grain size from grain growth after SRX (μm)					31.1	26.8	22.9	
		Retained strain after last pass at FMH						0.142
		Ferrite grain size from SRX population (μm) after cooling at 80°C s^{-1}						10.1
		Ferrite grain size from un-recrystallized population (μm) after cooling at 80°C s^{-1}						9.1
		Final ferrite grain size mix (μm)						9.7

- The model predicts no meaningful effect of the initial or entry austenite grain size in the slab (it was varied between 1200 and 200 μm in the model) on the final austenite or ferrite grain sizes.
- On all the HCR-slabs analysed, the retained strain after the last pass was generally between 0.15 and 0.1, leading to a finer ferrite grain size because of the additional driving force that is provided by this strain, i.e. 9.1 μm versus the 10.1 μm from the fully recrystallized material for the example shown at the bottom of Table IV. The ferrite grain structure of this strip is shown in Figure 7 indicating, even visually, the presence of a mixed grain size structure.
- Relatively little interpass grain growth is predicted with some grain size increase from this source predicted only after pass F4. This is not unusual as the interpass times become very short in a high speed tandem strip mill at those smaller grain sizes that would produce a reasonable driving force for grain growth. During the earlier passes (R1 to F3) the austenite grain size is still large and produces little driving force for grain growth.
- Using the same basic model but with only published constants from Table III for mostly CCR strip steels and not the own experimentally tested constants, the austenite grain size appeared to develop quite differently with a much quicker austenite grain size reduction to values of about 20 μm or less, typically already at passes F2 to F3 and with significantly more grain growth after the last few passes than found here. This proved the value of determining at least a few critical hot working constants experimentally for this steel rather than relying only on published values.

Figure 7 provides an indication of the mixed grain structure in the 2 mm plant produced strip steel of Table IV. Using the relationship of Thompson[21] to test for uniformity of a grain structure once more, the ratio of (largest grain

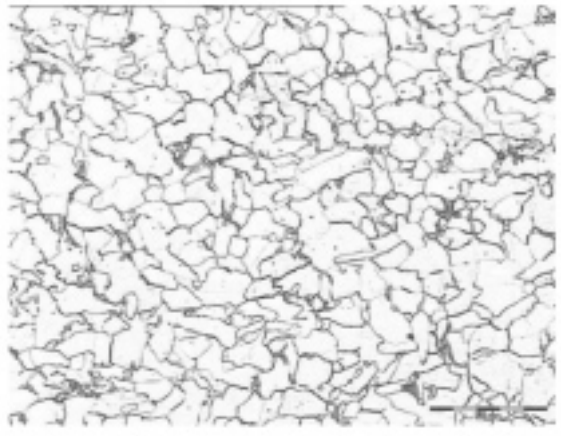

Figure 7—The non-uniform ferrite grain size distribution of the plant produced HCR-slab analysed in Table IV. Etchant used: 2% Nital. (Micrograph kindly provided by Verdoorn[34].)

diameter/mean intercept length) was found typically to be as high as 4 (compared to the ideal 1.86 for a fully uniform grain size distribution), indicating a highly non-uniform grain size structure for this hot rolled HCR-strip. This same ratio on an equivalent CCR-strip from ISCOR (Vanderbijlpark)[34], gave a typical value of the uniformity ratio of between 2.5 and 3, indicating a much more uniform grain size distribution in that material. This non-uniformity grain size effect in the HCR-strip, which was also found by Frawley *et al.*[2] in their HCR hot rolled laboratory samples, is probably due to the retained strain in the banded structure of the austenite at the point of transformation to ferrite, leading to a bi-modal grain size distribution in the hot rolled condition.

The austenite grain size development for the above reduction schedule is shown graphically in the Figure 8.

The predicted austenite grain size during passes F1 to F5 may be compared with a model developed by Muojekwu *et al.*[1] also for HCR-strip steel but with 0.17%C and 0.74%Mn (i.e. substantially higher carbon and manganese than were used in this study) that was equally rolled down in five finishing stages but with a final strip thickness of 2.87 mm instead of the present 2 mm of Figure 8. A direct comparison reveals that this model presented here predicts about 13 percent larger austenite grain sizes after F1 and F2, somewhat smaller grain sizes after F3 (25 percent smaller) and F4 (4 percent smaller) and a slightly larger grain sizes (23 μm versus the 20 μm of Muojekwu *et al.*) after F5. The substantial differences in alloy content and final thicknesses between the two HCR-products and processes, however, make direct conclusions from such a comparison uncertain.

Sensitivity effects of process changes

Temperature variations

The model may now be used to predict the sensitivity effects of different strategies in the design of the reduction schedule for this plant, for instance temperature changes or changes to the values of the reduction per pass. As a first example, consider a change in the temperature of the product along the entire line (i.e. from the reheat furnace to the finishing mill head or FMH) by a set value, say in intervals of 10°C. The effects of such a change in the process on the austenite grain size at the FMH, on the ferrite grain size in the final product and on the retained strain in the austenite just before transformation to the ferrite, are shown in Figure 9. The A_{r3} (or ferrite start temperature) at a cooling rate of 80°C/s in the SAE 1006 HCR-processed steel used for the hot deformation studies, has been measured[34] to be as low as 714°C or more than 180°C below the normal hot rolling finishing temperature of about 900°C.

The model shows that although the final austenite grain size may increase measurably with an increase in the temperature of the product along the entire line, this should have little effect on the final ferrite grain size. On the other hand, a slight decrease in the line's rolling temperatures from a normal level is probably also not so critical to the final ferrite grain size as long as the temperature does not drop below the A_{r3} before exiting from pass F5. In an ongoing parallel study on this same steel[34] it has been found that the HCR-strip generally has a much lower A_{r3} temperature than the equivalent CCR-strip.

Although the model presented here, may be in broad agreement with the analyses of the mill logs from the plant and also the measured final ferrite grain size, the fundamental question as to why two different temperature regimes were found in both the hot deformation tests and the mill log analyses, needs to be considered. Fundamentally, a change in activation energy of any thermally activated process usually signals a change in rate controlling mechanism. It is believed that DRX is controlled by a Bailey-Hirsch,[35, 36] type of dynamic nucleation and growth of recrystallizing nuclei, as Kikuchi[37] has shown so elegantly in hot deformed Cu. The formation of a recrystallizing nucleus on a pinned grain boundary by the Bailey-Hirsch method is critically dependent on both the grain size and the pinning frequency and it is, therefore, understandable that the starting grain size D_0 appears in the expression for the critical strain to initiate DRX as was shown in Equation [2]. Some indication already exists that the pinning of grain

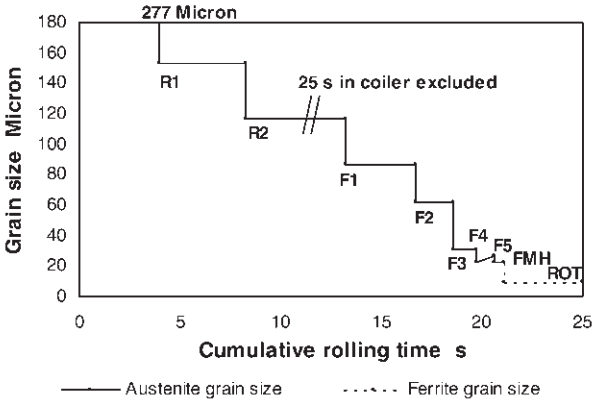

Figure 8—Austenite grain size development (R1 to FMH) shown for a 75 mm slab reduction to 2 mm hot rolled strip as well as the calculated final ferrite grain size (FMH to ROT) expected in the strip. FMH = Finishing Mill Head, and ROT = Run-out Table. Note that 25 seconds from the transfer bar's temperature equalization time in the coil box have been excluded from the accumulated time

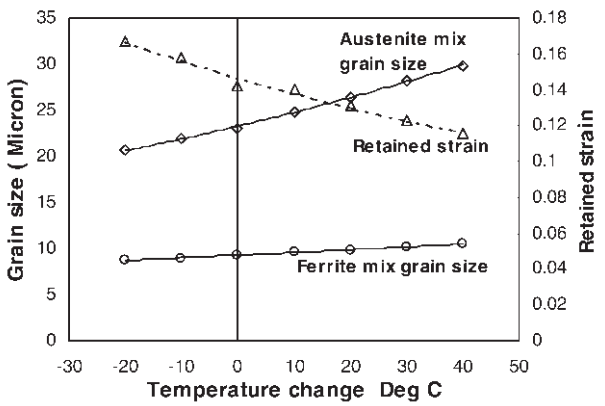

Figure 9—Sensitivity effects on the predicted austenite grain size at the FMH, on the predicted ferrite grain size after the FMH, and on the retained strain in the austenite just before transformation to ferrite, are shown as a function of changing the product/process temperatures along the entire line by a set amount

boundaries in the HCR-material studied here may be fundamentally different from that in an equivalent CCR-steel where it was found through Transmission Electron Microscopy investigations of the two steels[38] that the grain boundaries in hot rolled HCR-material were significantly pinned and presented a pronounced 'wavy' appearance, whereas those in the equivalent CCR-material showed little evidence of strong pinning and were generally straight. These observations, however, apply to the hot rolled ferrite microstructure and it remains uncertain whether this would also be found in the austenite.

In fact, Muojekwu *et al.*[1] also address this same uncertainty of the respective contributions of temperature and austenite grain size on their HCR-steel through proposing a combined temperature and grain size effect (with different grain size and temperature dependencies below 244 μm and above this cut-off grain size) for the decision of whether DRX will take place or not during hot deformation, i.e. a somewhat different approach than that used here from Equation [2]. It is further interesting to note that they also found a much smaller temperature dependence or activation energy for DRX at larger grain sizes than the 312 kJ/mol that is usually quoted in the literature (although their value is again significantly smaller than the lower value of 238 kJ/mol even found in this study). These authors, therefore, (as also most other workers) follow a prudent approach by defining their activation energies derived from hot work studies as 'apparent activation energies' and do not attempt to assign any specific deformation and softening mechanism to the results.

In most hot deformation studies on creep resistant steels, it has been found that the activation energy for hot deformation is up to 50 percent greater than that for self-diffusion or creep[39] and this general discrepancy has defied any satisfactory explanations based on existing models for deformation at elevated temperatures[40]. A direct comparison between the activation energy found by Muojekwu *et al.* and this work is also probably not quite valid due to the different approaches used in testing for DRX and also because of the rather large differences in alloy content between the two sets of HCR-materials with 0.17%C and 0.74%Mn in their steel versus the 0.038%C and 0.25%Mn in the steel used for this work. It is clear, however, that many questions still remain in the area of an apparent low activation energy for HCR-material with large grain sizes and tested at higher temperatures versus a higher activation energy at lower temperatures on smaller grain size HCR-material.

Variations in the reduction schedule

Similarly one may predict the sensitivity effects of a change in reduction schedule on the final ferrite grain size. From Table I, it may be concluded that higher than average reductions per pass are applied in the four passes R1 to F2 (where the product temperatures are still high and DRX is taking place with a lower MFS in the steel) and lower than average reductions per pass are applied in the last three passes of F3 to F5. Consider now the sensitivity of the process to a fixed and equal percentage decrease (or increase) in reduction per pass over the last three passes (F3 to F5) while transferring this decreased (or increased) reduction from these three passes evenly to the first four passes to maintain the total strain from 75 mm slab to 2 mm strip constant. The sensitivities to such changes in the reduction schedules of the austenite grain size at the FMH, the ferrite grain size after the FMH, and the retained strain at the FMH are shown in Figure 10.

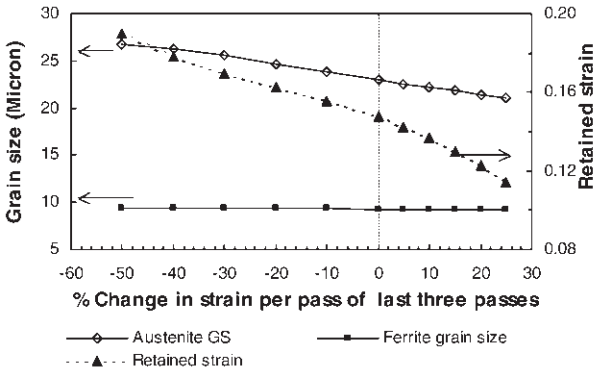

Figure 10—Sensitivity analysis of changing the reductions per pass of the three last passes (F3 to F5) by an equal percentage and transferring these changes evenly to the remaining first four passes (R1 to F2) to maintain a constant total reduction from the 75 mm slab to a 2 mm strip

Once more, the model of this HCR-process predicts that such changes to the reduction schedule are likely to be marginally effective in changing the austenite grain size and the retained strain but would be very ineffective in changing the ferrite grain size in the final hot rolled strip. In fact, considering both Figures 9 and 10 it appears that this particular HCR hot rolling process is likely to be a very stable one in terms of the ferrite grain size in the final strip, with little sensitivity towards variations in temperature and strain per pass of the last three reduction passes.

Conclusions

- Both mill log analyses and hot deformation studies have shown that the HCR hot rolled SAE 1006 strip steel from ISCOR (Saldanha) exhibits a two-stage hot working behaviour. Firstly, an apparent lower activation energy (238 kJ.mol^{-1}) for softening by DRX at temperatures above about 1000°C in the HCR-steel with an as-cast or large starting austenite grain size of 227 μm and secondly, an activation energy of about 330 kJ.mol^{-1} for SRX softening of the same material but at lower temperatures and with a smaller starting austenite grain size of 26 μm. As Muojekwu *et al.*[1] also found this two-stage effect on their HCR-processed low carbon manganese steel, it may appear to be a characteristic of this type of material.
- Some further constitutive constants for the softening by DRX have also been determined for this steel and these appear to fall largely within the range of constants determined by other workers for conventionally processed low carbon strip steels.
- A model for the development of the austenite and the final ferrite grain sizes of HCR hot rolled SAE 1006 strip steel from this plant and using a combination of own constants and published constants, has been developed and appears to provide a ferrite grain size in good agreement with plant data.

- The model used for the production practice at the time of the study also predicts complete softening through dynamic recrystallization during passes R1 to F2 but incomplete static recrystallization in between the passes F3 to the FMH, and this results in some retained strain in the austenite as it transforms to ferrite, generally leading to a smaller ferrite grain size in the final strip.
- The model predicts relatively little effect on the final ferrite grain size of any changes in the hot rolling temperatures or the strain per pass in passes F3 to F5.
- In a parallel study to this work[41], the austenite to ferrite transformation behaviour of these HCR and CCR strip steels are being compared and it already appears that changes to the run-out table cooling process and possibly the subsequent coiling process may have a more significant effect than any process changes in the hot rolling parameters.
- Comparison of plant-processed highly HCR and CCR strip steel samples from ISCOR, revealed a more non-uniform ferrite grain size distribution in the HCR-material, an observation that confirms a finding by Frawley *et al.*[2] on their laboratory hot rolled HCR low carbon manganese steel samples. This, therefore, also may appear to be a characteristic of this type of material processed by the HCR route and possibly arises from incomplete SRX taking place during the last few passes in a typical compact strip plant.

Acknowledgements

ISCOR (Saldanha Steel) kindly supplied the mill logs and the experimental materials, Mr Francois Verdoorn of the Industrial Metals and Minerals Research Institute of the University of Pretoria assisted from time to time with the hot working tests, and many helpful discussions on hot deformation were held with Dr Kevin Banks of the same institute. The valuable assistance of Prof. GT van Rooyen and Mr Charl Smal of the University in modifying the apparatus for the hot working tests is also greatly appreciated. Hot rolling of the as-cast structure was done by MINTEK and their assistance is kindly acknowledged. Mr Johan Bornman of the University was responsible for optimizing the austenite grain boundary decoration technique through hyper-eutectoid carburization and his and Mr Joel Matea's kind assistance in the sample preparation is also appreciated. The permission of the University of Pretoria and of ISCOR in allowing publication of this work is kindly acknowledged.

References

1. Muojekwa,C.A., Jin, D.Q., Samarasekera, I.V., and Brimcombe, J.K. Thermomechanical History of Steel Strip During Hot Rolling—A Comparison of Conventional Cold-Charge Rolling and Hot-Direct Rolling of Thin Slabs, *37th MWSP Conference Proceedings*, ISS, 1996, vol. XXXIII, pp. 617–631.
2. Frawley, L.D., Priestner, R. and Hodgson, P.D. *THERMEC 907: Int. Conf. On Thermomechanical Processing of Steels and Other Materials*, T. Chandra and T. Sakai, (eds.). The Minerals and Metals Soc. US, 1997, pp. 2169.
3. Sims, R.B. *Proc. Inst. Mech. Eng.*,1954, vol.168, p 191.
4. Hitchcock, J.H. *Roll Neck Bearings*, Appendix I, ASME New York, 1953, pp. 33.
5. Hosford, W.F. and Caddell, R.M. *Metal Forming: Mechanics and Metallurgy*, 2nd. edition, PTR Prentice Hall, Englewood Cliffs, 1993, pp. 222.
6. *Theory and Practice of Flat Rolling*, ISIJ (ed.), ISIJ Tokyo, 1984, p. 7.
7. Siciliano, F., Minami, K., Maccagno, T.M., and Jonas, J.J. *ISIJ International*, 1996, vol. 36, pp. 1500–1506.
8. Misaka, Y., and Yoshimoto, T. *Journ. Japan Soc. Technology of Plasticity*, 1967-8, vol.8, p. 414.
9. Sellars, C.M. *Proc. Int. Conf. on Hot Working and Forming Processes*, July 17-20, 1980. (eds.) CM Sellars and CJ Davies. Metals Soc. of London, pp. 3-15.
10. Sellars, C.M., *Mater. Sci. Technology*, 1985, vol. 1, pp. 325-332.
11. Beynon, J.H.,Brown, P.R., Mizban, S.I., Ponter, A.R.S., and Sellars, C.M. *Proc. of NUMIFORM Conf.*, Gothenburg, Sweden, Aug. 25-29, 1986. K Mattiasson, A Samuelsson, RD Wood and OC Zienkiewicz (eds.). AA Balkema, Rotterdam, Holland, pp 213–18.
12. Sellars, C.M., and Whiteman, J.A. *Met. Sci*. 1979. Mar.–Apr., pp. 187–194.
13. Sellars, C.M. *Int. Conf. On Physical Metallurgy of Thermomechanical Processing of Steels and Other Metals THERMEC 88*, Tokyo, June 6–10, 1988. I Tamura (ed.). Iron and Steel Inst. Japan, Tokyo, pp. 448-457.
14. Samarasekera, I.V., and Hawbolt, E.B. Overview of modelling the microstructural state of steel strip during hot rolling. *The Journ. of the South African Inst. of Mining and Metallurgy*, July/August 1995, pp. 157–165.
15. Garafolo, F. *Fundamentals of Creep and Creep Rupture of Metals*, MacMillan, New York, 1965.
16. Sellars, C.M., and McTegart, W.J. *Mem. Sci. Rev. Met.*, 1966, vol. 63, pp. 731–446.
17. Sellars, C.M., and Whiteman, J.A. *Met. Sci.*, 1979, vol. 13, pp. 187–194.
18. Zener, C., and Holloman, J.H. *Journ. Appl. Phys.*, vol. 15, 1944, p. 22.
19. L.S. Darken, L.S., Smith, R.P., and Filler, E.W. *Trans. AIME.*, 1951, vol.191, p. 1174.
20. ASTM Specification E 112 of 1982, part 11, p. 167.
21. Thompson, A.W. Calculation of the True Volume Grain Diameter, *Metallography*, 1972, vol.5, pp. 366–369.
22. Gleeble 1500^{TM}, *Operational Manual*, Dynamic Systems Inc., US.
23. Uvira, J.L. and Jonas, J.J. *Trans. Met. Soc. AIME.*, 1968, vol. 242, pp. 1619–1627.
24. Jonas, J.J., Axelrad, D.R., and Uvira, J.L. Proc. *Int. Conf. on the Strength of Metals and Alloys*, Tokyo, September 1967, Trans. Japan Inst. Metals, 1968, vol. 9 supplement, pp. 257–267.
25. Dieter, G.E. *Mechanical Metallurgy*, 1988, McGraw-Hill, SI Edition, 541 pp.
26. Rowe, G.W. *Principles of Metalworking*, 1965, Edward Arnold, London.
27. Richardson, G.J., Hawkins, D.N., and Sellars, C.M. *Worked Examples in Metalworking*, 1985, Inst. of Metals, London, p. 33.
28. McQueen, H.J., and Ryan, N.D., *Matls. Science and Eng.*, 2002, vol. A322, pp. 43–63.
29. Devadas, C., Barager, D., Ruddle, G., Samarsekera, I.V., and Hawbolt, E.B. *Metallurgical Trans*. A, 1991, vol. 22A, pp. 321–333.
30. Jonas, J.J. *ISIJ Int.*, 2000, vol. 40, pp. 731–738.
31. Anelli, E. *ISIJ Int.* 1992, vol. 32, pp. 440–449.
32. Bowden, J.W., Samuel, F.H., and Jonas, J.J., *Metallurgical Trans.*, 1991, vol. 22A, pp. 2947–2957.
33. Perdix, C.H. Characteristic of Plastic Deformation of Metals during Hot Working, Report CECA No. 7210 EA/311, 1987, Saint Germain-en-Laye (France), Inst. de Recherches de la Siderurgie Francaise (IRSID).
34. Verdoorn, F. IMMRI, University of Pretoria, unpublished work, 2002.
35. Bailey, J.E. *Phil. Mag.*, 1960, vol. 5, pp. 833.
36. Bailey, J.E., and Hirsch, P.B. *Proc. Roy. Soc.*, 1962, vol. A267, pp. 11.
37. Kikuchi, S. and quoted by T. Sakai and J.J. Jonas. Acta. Met., 1984, vol. 32, p. 189.
38. Tuling, A. IMMRI, University of Pretoria, unpublished work, 2001.
39. Jonas, J.J.,Sellars, C.M., and McTegart, W.J. *Met. Rev.*, vol. 14, 1969, p. 1.
40. Roberts, W. *Dynamic Changes that occur during Hot Working and their significance regarding Microstructural Development and Hot Workability*, G Krausz (ed.), ASM Metals Park, Ohio, US, 1983, p. 109.
41. Verdoorn, F. and Stumpf, W.E. to be published.

Appendix 1: Equations used for mill log analyses

Eq. No.		EQUATIONS	DEFINITIONS
		Sims Working rolls corrective equations	
1 2	Flattened work roll radius	$R' = R\{1 + (C\,P)/w\,\Delta h\}$ $C = \frac{16(1-\nu^2)}{\pi E}$	R′ = flattened work roll radius (mm) R = nominal radius (mm) ν = Poisson's ratio E = Young's modulus of outer skin of roll material (GPa) P = roll force (N) w = width of plate (mm) Δh = (H-h) = thickness reduction (mm)
3 4	Redundant strain	$\varepsilon_r = \frac{(H-h)}{4\sqrt{4(R')^2\sin^2(\alpha/2) - (H-h)^2/4}}$ $\alpha = \arccos[1 - \{(H-h)/2R'\}]$	H = entry thickness (mm) h = exit thickness (mm) R′ = flattened roll radius (mm)
5 6	Forward Slip Ratio (FSR)	$V_e = V_r[1 + \{(2R'/h)\cos\phi_n - 1\}\{1 - \cos\phi_n\}]$ $\phi_n = \{h/R'\}^{1/2}\tan[(\pi/8)(h/R')^{1/2}\ln(1-r) + \frac{1}{2}\tan^{-1}\{r/(1-r)\}^{1/2}]$	r = (H – h)/H V_e = exit strip speed (corrected for forward slip) in m/s V_r = tangential velocity of working roll = 2πR′U U = revolutions/sec of working roll
		Sims Mean Flow Stress calculations from mill log data	
7	Mean flow stress (Sims)	$MFS_{Sims} = \frac{P}{[(2/\sqrt{3})\,w\,\{R'(H-h)\}^{1/2}\,Q]}$ $Q = [(1/2)\{(1-r)/r\}^{1/2}\{K_3 - K_4\} - (\pi/4)]$ $K_3 = 2\pi K_2$ and $K_2 = [(1/2)\tan^{-1}\{r/(1-r)\}^{1/2}]$ $Y = [2R'\{1 - \cos\phi\} + h]$ $K_1 = (\pi/8)(h/R')^{1/2}\ln(1-r)$ $K_4 = \{R'/h\}^{1/2}\ln[(Y/h)^2(1-r)]$ $\phi = \{\tan(K_1 + K_2)\}\{h/R'\}^{1/2}$	MFS_{Sims} = mean flow stress according to Sims (MPa) P = roll force (MN) w = plate width (mm)
		Strain and strain rate equations	
8 9 10	Strain rate	$\dot{\varepsilon}_m = \frac{0.1048\,R'\,U\,\varepsilon_T}{\sqrt{(R'\Delta h)}}$ (FSR) $\varepsilon_T = (\varepsilon_n + \varepsilon_r)$ $V = (2\pi R'\,U)/60 = 0.1048\,R'\,U$ (m/s)	$\dot{\varepsilon}_m$ = corrected strain rate (/s) U = roll speed in RPM FSR = calculated Forward Slip Ratio ε_T = total strain per pass ε_n = nominal strain per pass ε_r = redundant strain per pass
11	Nominal strain per pass	$\varepsilon_n = \{2/\sqrt{3}\}\ln(H/h)$	$2/\sqrt{3}$ = Von Mises conversion for plane strain compression
12	Interpass times (s)	$t_{ip} = Y\,(SF)/V_r$	Y = interpass distance (m) SFR = Forward Slip Ratio V_r = peripheral roll speed (m/s)
		Misaka Mean Flow Stress calculations for SRX	
13 14 15	Misaka MFS for SRX of C–Mn steels	$MFS_M = (f_1)(f_2)\,9.8\exp\{0.126 - 1.75[C] + 0.0594[C]^2 + \frac{(2851 + 2968[C] - 1120[C]^2)}{(T+273)}\}$ $f_1 = (0.768 + 0.137[Mn] + 0.51[Nb] + 4.217[Ti])$ $f_2 = (\varepsilon_{pass})^{0.21}(\dot{\varepsilon}_{pass})^{0.13}$	MFS_M = mean Flow Stress MPa [C] = mass% Carbon T = temperature °C [Mn] = mass% Mn [Nb] = mass % Nb [Ti] = mass % Ti ε_{pass} = strain per pass $\dot{\varepsilon}_{pass}$ = strain rate per pass /s
16	Misaka MFS corrections for constant strain and strain rate per pass	$MFS_{corr} = MFS_{Sims}\{\varepsilon_{const}/\varepsilon_{act}\}^{0.21}\{\dot{\varepsilon}_{const}/\dot{\varepsilon}_{act}\}^{0.13}$	MFS_{Corr} = corrected MFS_{Sims} for a constant strain (ε_{const}) and strain rate ($\dot{\varepsilon}_{const}$) per pass with an actual strain (ε_{act}) and strain rate ($\dot{\varepsilon}_{act}$) per pass

Appendix 2: Decision-making flow chart for calculating the austenite grain size development during hot rolling

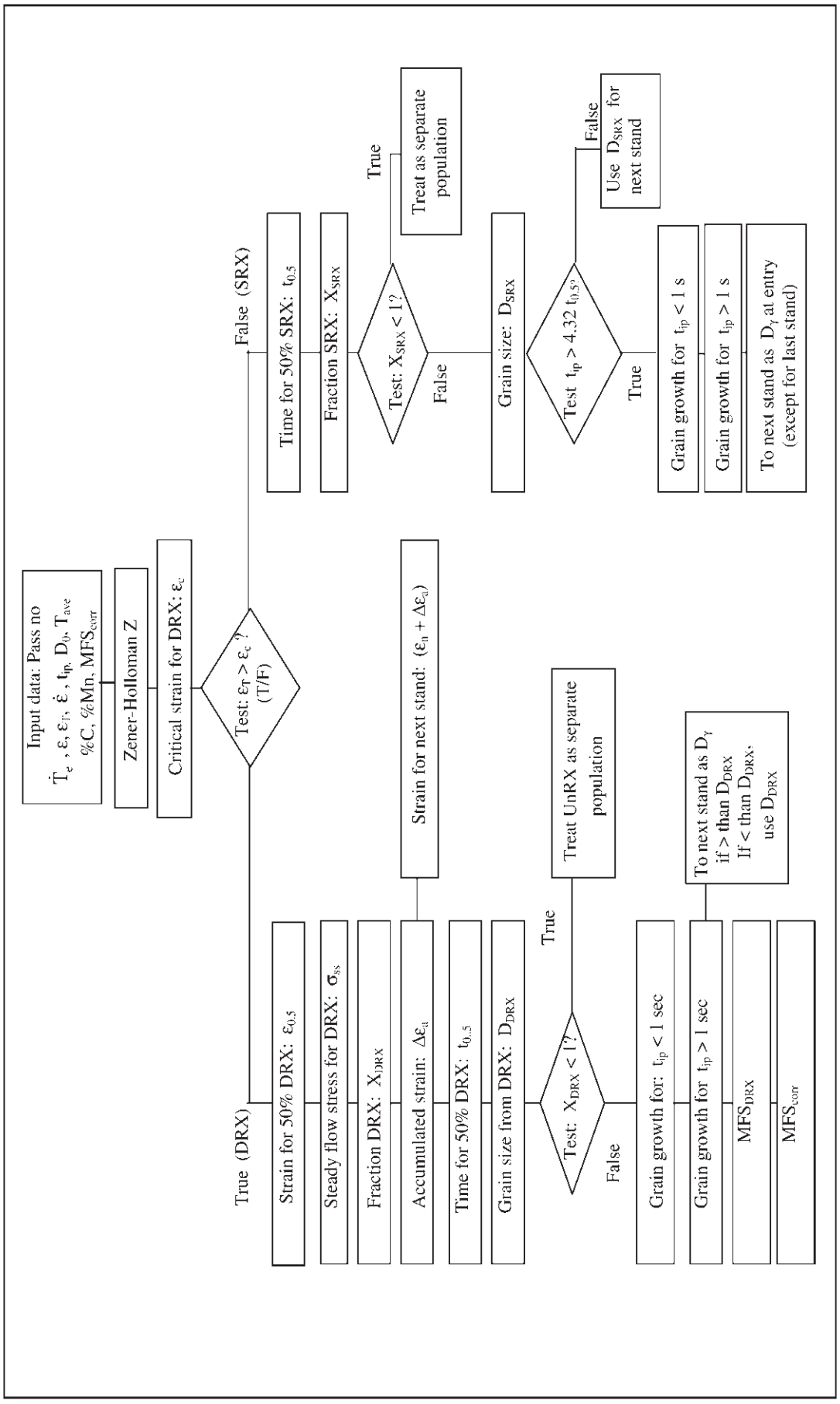

Appendix 3: Constitutive equations used in the austenite and ferrite grain size development model

Eq. No.	Area of application	Equation	Definitions
		Constitutive equations for dynamic recrystallization	
17 18 19	Test for DRX	$\varepsilon_p = A_1 (D_0)^{0.3} Z^q$ Above 1000°C and with D_0=277 µm : $Z_1 = \dot{\varepsilon}\ \exp [238000/RT]$, $A_1 = 6.2x10^{-4}$, q =0.22 Below 1000°C and with D_0=26 µm : $Z_2 = \dot{\varepsilon}\ \exp [330000/RT]$, $A_1 = 1.3x10^{-4}$, q = 0.2	ε_c = critical strain for DRX = 0.8 ε_p where ε_p = peak strain D_0 = austenite grain size going into stand (µm) T = temperature °K Z = Zener-Holloman parameter (/s) R = universal gas constant (J/mol/°K) $\dot{\varepsilon}$ = strain rate during pass
20	Strain at 50% DRX	$\varepsilon_{0.5} = 1.144x10^{-5} (D_0)^{0.28} (\dot{\varepsilon})^{0.05} \exp[53388/RT]$	
21	Fraction from DRX	$X_{DRX} = 1 - \exp[-0.693\{(\varepsilon_T - \varepsilon_c)/\varepsilon_{0.5}\}]$	X_{DRX} = fraction recrystallized from DRX ε_T = total strain of pass (including redundant strain)
22 23	Mean flow stress from DRX	Above 1000°C: $\sigma_{ss} = 69.93[\sinh^{-1}\{(Z_1/3.8x10^8)^{0.19}\}]$ Below 1000°C: $\sigma_{ss} = 69.93[\sinh^{-1}\{(Z_2/1.25x10^{13})^{0.2}\}]$	σ_{ss} = Flow stress from DRX (MPa)
24 25	Accumulated strain and strain for next stand	$\Delta\varepsilon_a = K_{acc} (1 - X_{DRX}) \varepsilon_{n-1}$ $\varepsilon_{n+1} = \varepsilon_n + \Delta\varepsilon_a$	$\Delta\varepsilon_a$ = accumulated strain for stand n K_{acc} = constant 0.5 to 1 ε_{n-1} = strain from previous stand ε_{n+1} = strain for next stand
26	Time for 50% DRX	$t_{0.5} = 0.4\ \{\dot{\varepsilon}\ \exp(238000/RT)\}^{-0.8}\ \{\exp(240000/RT)\}$	$t_{0.5}$ = time for 50% DRX (s)
27	Grain size from DRX	$D_{DRX} = 2.6x10^4\{\dot{\varepsilon}\ \exp(238000/RT)\}^{-0.23}$	D_{DRX} = grain size from DRX (µm)
28	Grain growth after DRX at $t_{ip} < 1$ s	$(D_{gg})^2 = (D_{DRX})^2 + 1.2x10^7\ \{(t_{ip} - 2.65t_{0.5})\exp(-113000/RT)\}$	D_{gg} = grain size after t_{ip} (µm)
29	Grain growth after DRX at $t_{ip} > 1$ s	$(D_{gg})^7 = (D_{DRX})^7 + 8.2x10^{25}\ \{(t_{ip} - 1) - 2.65t_{0.5}\}\{\exp(-400000/RT)\}$	D_{gg} = grain size after $(t_{ip} - 1)$ (µm)

Constitutive equations for static recrystallisation			
30	Time for 50% SRX	$t_{0.5} = 2.3x10^{-15}\ \varepsilon^{-2.5}\ (D_\gamma)^2\ \exp(230000/RT)$	$t_{0.5}$ = time for 50% recrystallization by SRX D_0 = austenite grain size at t = 0 (μm)
31	Fraction recrystallized by SRX	$X_{SRX} = 1 - \exp\{-0.693(t_{ip}/t_{0.5})\}$	X_{SRX} = fraction recrystallized by SRX t_{ip} = interpass time (sec)
32	Grain size from SRX	$D_{SRX} = 343\ (D_0)^{0.4}\ \varepsilon^{-0.5}\ \exp(-45000/RT)$	D_0 = austenite grain size at t = 0 (μm)
33	Grain growth from SRX for $t_{ip} < 1$ s	$(D_{gg\ SRX})^2 = (D_{SRX})^2 + 4.0x10^7\{t_{ip} - 4.32t_{0.5}\}\{\exp(-113000/RT)\}$	$D_{gg\ SRX}$ = austenite grain size after time of t_{ip} (μm)
34	Grain growth from SRX for $t_{ip} > 1$ s	$(D_{gg})^7 = (D_{gg\ SRX})^7 + 1.5x10^{27}\{(t_{ip} - 1) - 4.32t_{0.5}\}\{\exp(-400000/RT)\}$	D_{gg} = grain size after grain growth at times $t_{ip} > 1$ s $D_{gg\ SRX}$ = grain size after 1 s of grain growth
35	Retained strain from incomplete SRX over last three passes	$\varepsilon_r = [X_3X_4(1-X_5)\varepsilon_5] + [X_3(1-X_4)(1-X_5)(\varepsilon_4+\varepsilon_5)]$ $+ [(1-X_3)X_4(1-X_5)\varepsilon_5] + [(1-X_3)(1-X_4)(1-X_5)(\varepsilon_3+\varepsilon_4+\varepsilon_5)]$	Eq.takes strain-on-strain into account for all values of $X < 1$ over the last three passes. X_n = fraction recrystallized by SRX after pass n and ε_n = actual true strain per pass of the n-th pass
Constitutive equations for the transformation from austenite to ferrite			
36	Nucleation of ferrite grains from recrystallized austenite (no retained strain)	$D_{\alpha\ SRX} = \{6.77 - 10[C] - [Mn]\}\{C_R^{-0.175}\}\{D_{gg}^{0.4}\}$	$D_{\alpha\ SRX}$ = α grain size from SRX aust. (μm) D_{gg} = austenite γ grain size from prior grain growth (μm) C_R = cooling rate in °C/s [C] and [Mn] = carbon and manganese (wt%) in the steel
37	Nucleation of ferrite grains from unrecrystallized austenite grains with retained strain	$D_{\alpha\ UnSRX} = \{6.77 - 10[C] - [Mn]\}\{C_R^{-0.175}\}\{D_{gg}^{(0.4-0.25\varepsilon)}\}$	$D_{\alpha\ UnSRX}$ = ferrite grain size from unrecrystallized austenite grains (μm) ε = retained strain in the unrecrystallized austenite grains of equivalent size to $D_{\alpha\ SRX}$
38	Weighted average of ferrite grain size after transformation from austenite	$D_\alpha = D_{\alpha\ SRX}\ X_{SRX} + D_{\alpha\ UnSRX}\ \{1 - X_{SRX}\}$	